Trehalose Prevents Myoglobin Collapse and Preserves Its Internal Mobility†

G. Madhavi Sastry and Noam Agmon*

Department of Physical Chemistry and the Fritz Haber Research Center, The Hebrew University, Jerusalem 91904, Israel

Received October 17, 1996; Revised Manuscript Received January 23, 1997⊗

ABSTRACT: A quantitative model, which involves diffusion on a temperature-dependent potential, is utilized to analyze the time-dependence of geminate CO recombination to sperm whale myoglobin in a trehalose glass and the accompanying spectral shifts. Most of the recombination is inhomogeneous. This is due to higher geminate reactivity rather than slower protein relaxation. A fraction of the hemes undergoes relaxation with a concomitant increase in the barrier height for recombination. The activation energy for conformational diffusion (relaxation) is considerably lower than in glycerol/water. "Protein collapse", manifested in glycerol/water by a decrease in the equilibrium conformational separation between the bound and deoxy states, is completely prevented in trehalose. We postulate that the high internal viscosity in glycerol/water is due to dehydration of the heme pocket. Trehalose prevents the escape of the few vital internal water molecules and thus preserves the internal lability of the protein. This might be important in understanding the ability of trehalose to protect against the adverse effects of dehydration.

1. INTRODUCTION

Water is essential for normal protein function (Edsall & McKenzie, 1983; Rupley & Careri, 1991; Rand, 1992). Dehydration can lead to sizable, partially irreversible, conformational changes in some proteins (Prestrelski *et al*., 1993): very labile proteins such phosphofruktokinase (PFK)[1] denature and lose their activity in the dried state; dry lysozyme unfolds but may refold during rehydration; the polypeptide poly-L-lysine undergoes a transition into a β-sheet conformation to maximize internal hydrogen bonds upon dehydration.

In spite of that, pollen, seeds, fungal spores, and a variety of microscopic animals can survive dehydration for decades and restore activity within minutes of rehydration, a phenomenon known as "anhydrobiosis" (Crowe *et al*., 1992). The secret of revival appears to lie in high concentrations of sugars: sucrose in seeds of higher plants and a disaccharide, trehalose, in the lower organisms. The latter seems to be significantly more effective in preventing the adverse effects of dehydration. For example, PFK, which completely inactivates after dehydration, restores 100% of its activity when rehydrated following a freeze-dry process in the presence of trehalose, but only 13% of the original activity is restored if trehalose is replaced by glucose (Carpenter *et al*., 1987).

Experiments with the model peptide, poly-L-lysine, indicate that the conformational transition into its β-sheet form is inhibited in the presence of sucrose trehalose, and it retains its solution structure in the dried state (Prestrelski *et al*., 1993). FTIR spectroscopy of lysozyme indicates that characteristic IR bands that are either lost or shifted upon dehydration (most notably the amide II and carboxylate bands) are re-established for lysozyme freeze-dried in the presence of trehalose (Carpenter & Crowe, 1989). This spectrum differs significantly from that of the crystallized sugar, indicating that the sugar might replace water molecules in forming hydrogen bonds to the surface of the protein.

This "water replacement hypothesis" (Prestrelski *et al*., 1993; Carpenter & Crowe, 1989) cannot explain the superior protecting efficiency of trehalose compared to glucose against PFK dehydration (Carpenter *et al*., 1987). It also does not explain why the sugar's protection ability reaches a maximum at about 100 mM sugar. Also, while the hypothesis is reasonable for water-binding sites at the protein surface it is less plausible for internal water molecules. For example, the oxygen-storing protein myoglobin (Mb) has several internally bound water molecules. One of these apparently binds to the distal histidine in the deoxy state (Cheng & Schoenborn, 1990, 1991; Lounnas *et al*., 1992, 1994). In addition, there are mobile water molecules in the ligand entry channel that are seen in molecular dynamics simulations (Lounnas *et al*., 1994) but not in neutron diffraction (Cheng & Schoenborn, 1991). It seems quite unlikely that a bulky trehalose molecule would enter into these confined regions of the protein.

It was shown that trehalose has a significantly higher glass transition temperature than glucose and other sugars (Green & Angell, 1989; Crowe *et al*., 1996). In a freeze-dry procedure it would glassify at higher water contents where its osmotic pressure is expected to be lower. An interesting possibility is that this property of trehalose prevents the loss of *internal* water molecules. The present work provides evidence for such an "internal water hypothesis" from MbCO kinetics. These internal water molecules, together with the surface hydration water, are apparently vital for preserving the internal mobility of a protein (Doster *et al*., 1986).

To what extent is the internal protein mobility coupled to the external solvent/glass dynamics? Two opposing views are expressed in the heme protein literature. The study of Hagen *et al*. (1995, 1996), whose data we analyze below,

† Work supported by the U.S.−Israel Binational Science Foundation (BSF), Jerusalem, Israel, and the Zevi Hermann Schapira Research Fund. The Fritz Haber Research Center is supported by the Minerva Gesellschaft für die Forschung mbH, München, FRG.

⊗ Abstract published in *Advance ACS Abstracts,* May 15, 1997.

[1] Abbreviations: DSC, differential scanning calorimetry; Hb, hemoglobin; His, histidine; KHB, kinetic hole burning; Leu, leucine; Mb, myoglobin; PFK, phosphofruktokinase; SVD, singular value decomposition; sw, sperm whale.

S0006-2960(96)02605-0 CCC: $14.00

suggests that the enormous trehalose viscosity arrests all protein motion. The protein relaxation rate is assumed, following Kramers, to be inversely proportional to the sum of the protein and solvent friction (Ansari *et al*., 1992). Thus in viscous solvents (and certainly in glasses) protein relaxation is totally controlled by solvent viscosity. In contrast, the analyses of MbCO kinetics in glycerol/water solutions by Doster *et al*. (1993) and ourselves (Agmon & Sastry, 1996) suggest that the protein relaxation process, which is responsible for the increase in the innermost barrier height for rebinding (Agmon & Hopfield, 1983; Steinbach *et al*., 1991), is internal and mostly decoupled from the protein surface.

A related question is to what extent does the protein itself behave like a glass? Several dynamic studies of heme proteins suggest that protein relaxation is similar to the primary, α-relaxation of glasses (Iben *et al*., 1989; Frauenfelder *et al*., 1991; Parak & Frauenfelder, 1993). Glass-forming systems are characterized by a jump in the heat capacity at the glass transition temperature, T_g, non-exponential relaxation, and non-Arrhenius temperature-dependence of the relaxation rate parameter (Green *et al*., 1994). It has thus been assumed that proteins must also exhibit non-exponential non-Arrhenius relaxation (Steinbach *et al*., 1991), in contrast to the model employed in our work (Agmon & Sastry, 1996). However, recent differential scanning calorimetry (DSC) studies of hydrated Mb samples (Doster *et al*., 1986; Green *et al*., 1994; Sartor *et al*., 1994, 1995) cast doubts on the simplisitc analogy between glasses and proteins. These samples, which contain hydration but no bulk water, exhibit such a broad range of protein relaxation times that no glass transition temperature can be discerned in them (Sartor *et al*., 1994). The broad transition range may be reflect an inhomogeneous system in which individual relaxations are exponential and Arrhenius (Richert, 1994; Ediger *et al*., 1996).

The present analysis of MbCO kinetics in trehalose (Hagen *et al*., 1995, 1996), a continuation of our earlier analysis of MbCO in glycerol/water solutions (Agmon & Sastry, 1996), suggests a way to reconcile the seemingly conflicting evidence. We recognize two components that affect the CO-binding kinetics: a static one and a dynamic one. In 75% glycerol/water, the static component is responsible for a less reactive state of the photodissociated protein above the solvent glass transition. The "protein collapse" phenomenon (Agmon & Sastry, 1996) seems to be "slaved" (Iben *et al*., 1989) to the solvent glass transition and might indeed be driven by external viscosity (Ansari *et al*., 1992). It is completely eliminated in the trehalose glass. In contrast, the dynamic protein relaxation process becomes *faster* in trehalose, which can only be understood if it is decoupled from the protein surface (Doster *et al*., 1993; Agmon & Sastry, 1996).

This paper is structured as follows: first we overview the intricacies of the ligand-binding kinetics (Section 2). We then recount the quantitative theory that allows these data to be analyzed up to the onset of ligand escape (Section 3). We present the analysis of MbCO kinetics in trehalose as compared the glycerol/water data (Section 4). Finally, the questions raised in this Introduction are discussed in light of the new findings.

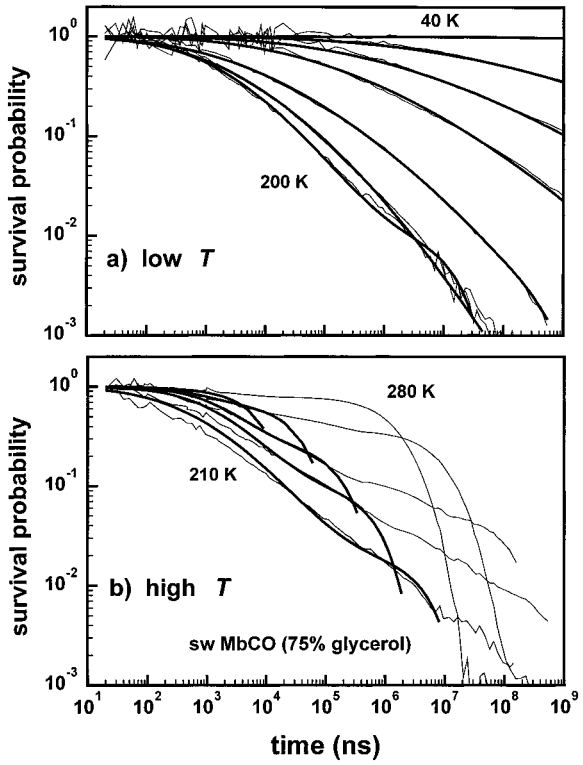

FIGURE 1: CO binding to sperm whale myoglobin in 75% glycerol/water solutions. Experimental data: thin curves (Post *et al*., 1993). (a) Low-temperature regime: temperatures (top to bottom) are 40, 80, 100, 120, 150, 180, and 200 K. (b) High-temperature regime: temperatures (top to bottom) are 280, 250, 230, 220, and 210 K. Bold curves are fits to the model of eqs 11 and 14. Parameters are collected in Table 1 and in Figures 5 and 6.

2. HEME−PROTEIN KINETICS

Low-temperature experiments first revealed the large extent of kinetic heterogeneity in MbCO (Austin *et al*., 1975). In these experiments, Mb is equilibrated in a glass-forming solvent, typically 75% glycerol/water, in the presence of CO and then cooled to the desired temperature, T. A fast (ns) laser flash dissociates the bound ligand. (As opposed to oxygen, CO has a near-unity dissociation yield.) Spectral differences between the bound and unbound states of Mb, e.g., in the Soret region, allow to monitor the "survival probability", $S(t)$, of the unbound heme by transient absorption. The heme eventually rebinds a CO molecule, either geminately or bimolecularly. However, this process can occur (depending on T) anytime between 10 ns and hundreds of seconds. The huge temperature and time ranges of these experiments make quantitative analysis a challenge.

A detailed review of heme−protein kinetics has recently been published (Sage & Champion, 1996). In the following we survey experimental and theoretical observations which could be relevant to our study of solvent effects on the heme relaxation mode. An example of sperm whale MbCO kinetics in glycerol/water, measured by Post *et al.* (1993), is shown in Figure 1. The low-temperature data in panel a are non-exponential but do speed up with increasing T in the usual fashion. The non-exponentiality could be explained by a distribution of rate coefficients arising from an inhomogeneous distribution of protein conformations (Austin *et al*., 1975).

At the higher temperatures, panel b, only the initial phase is due to distributed, inhomogeneous kinetics. At longer

times, conformational interconversion is faster than ligand binding and eventually $S(t)$ decays exponentially. At intermediate times an interesting "inverse temperature effect" is observed: CO binding *slows down* with increasing temperature. In glycerol/water, the temperature at which this reversal occurs is close to the solvent glass transition, ca. 190 K. This could create an impression that it is "slaved" to the solvent glass transition (Iben *et al*., 1989). We will demonstrate below that only the static, but not the dynamic, component of the inverse temperature effect is coupled to the solvent.

How does the transition from inhomogeneous to homogeneous kinetics occur (Agmon *et al*., 1994)? Initially it was thought that the kinks and bends observed in the rebinding curves reflect ligand migration within the protein matrix (Austin *et al*., 1975). It was subsequently suggested (Agmon & Hopfield, 1983) that protein relaxation, following ligand photolysis, will both homogenize the sample and increase the barrier for rebinding. The dynamic barrier-height increase gives rise to the inverse temperature effect as confirmed by recent experimental work (Friedman, 1985; Steinbach *et al*., 1991; Petrich *et al*., 1991; Lambright *et al*., 1991; Nienhaus *et al*., 1992; Tian *et al*., 1992; Ansari *et al*., 1994; Sage *et al*., 1995; Franzen *et al*., 1995). From $S(t)$ one may determine the "onset" and "termination" of protein relaxation as the first maximum and minimum of the "B-function", $-\mathrm{d}\ln S(t)/\mathrm{d}\ln t$ (Agmon *et al*., 1994).

By introducing temperature-dependence into the effective two-dimensional potential of (Agmon & Hopfield, 1983), we were recently successful in obtaining a quantitative model (Agmon & Sastry, 1996) describing the first two phases of the ligand-binding reaction, namely, the inhomogeneous and relaxation phases. After the termination of relaxation the model, which does not allow for ligand diffusion within the protein, predicts faster rebinding than experimentally observed. According to the model, by the termination of relaxation the protein becomes homogeneous exhibiting rapid fluctuations which allow for ligand migration. Molecular dynamics simulations indeed show a series of cavities which fluctuate and interconnect due to protein motions (Carlson *et al*., 1996). Therefore the first two phases of ligand binding contain most of the information pertinent to static and dynamic interactions in the vicinity of the binding site.

Analysis of the first two phases of MbCO kinetics in 75% glycerol/water solutions revealed two new effects (Agmon & Sastry, 1996). First, we have found that the "inverse temperature effect" in this solvent is not exclusively dynamic, since the rebinding slows down already during the initial inhomogeneous phase. This is reflected in the temperature-dependence of x_0, the separation between the equilibrium conformations of bound and deoxy hemes. We observed that x_0 is approximately constant below the solvent glass transition and decreases sharply above it (Agmon & Sastry, 1996). This "collapse" of the protein potential could reflect long-range structural changes which (a) extend all the way to the protein surface (and is therefore sensitive to the solvent glass transition) and (b) are either slower or faster than the time scale of the rebinding experiments (and thus appear as a static effect). In a solvent like trehalose, whose T_g is way above room temperature (Crowe *et al*., 1996), one might expect to see no protein collapse, as verified below.

Secondly, the "diffusion coefficient" for protein conformational relaxation, D, was found to obey a linear Arrhenius relation, with a large activation energy, $E_D = 62$ kJ/mol, both below and above the solvent T_g. This suggests that the protein relaxation process responsible for increasing the innermost barrier is internal, localized near the active site, and not extending all the way to the protein surface (Agmon & Sastry, 1996). This agrees with an earlier conclusion of Doster and co-workers that "the protein internal transitions are decoupled from the surface of the protein" (Doster *et al*., 1993).

Recently, laser-flash initiated recombination of CO with myoglobin (Mb) and hemoglobin (Hb) has been carried out in the dried state (Doster *et al*., 1993) and in trehalose glasses containing only 3% water by weight (Hagen *et al*., 1995, 1996; Gottfried *et al*., 1996). One of the goals of the present work is to check whether the factors responsible for the "inverse temperature effect" are still operative in trehalose glasses. Hagen *et al*. have analyzed the transient Soret absorption of flash-photolyzed sperm whale (sw) MbCO in trehalose (Hagen *et al*., 1995, 1996) using a singular value decomposition (SVD) technique. The first two SVD components provide information on the rebound population and spectral shift, driven by either protein relaxation or an inhomogeneous, "kinetic hole burning" (KHB) process (Campbell *et al*., 1987; Agmon, 1988). These workers assumed that protein relaxation in trehalose is completely arrested, and they fitted both population decay and spectral shifts to an inhomogeneous sheme,

$$\mathrm{A}_i \leftrightarrow \mathrm{B}_i \leftrightarrow \mathrm{C}_i, \qquad i = \text{protein conformation} \qquad (1)$$

in which no interconversion within the A_i, B_i, or C_i manifolds is possible (Hagen *et al*., 1995, 1996).

The above assumptions are troubling in two respects: first, it is not clear that the external solution viscosity is a direct determinant of the internal protein viscosity. By analogy, there are huge differences in viscosity between a liquid inclusion within a solid rock and the surrounding rock. The decoupling of internal protein relaxation from the external glass is difficult to assess from bulk equilibrium DSC measurements, which will pick up enthalpy changes in both protein and glass, but could be deduced from a careful analysis of the transient spectroscopic data. Second, the inhomogeneous model of Hagen *et al*. assumes that the ligand escapes from the heme pocket of a *frozen* protein, to the states C_i in eq 1. This is in apparent contradiction with molecular dynamics evidence indicating that sizeable protein fluctuations are a prerequisite for ligand escape (Carlson *et al*., 1996).

The next section describes our quantitative model which is based on solving an equation of motion rather than fitting empirical stretched-exponential functions. It is a unified approach that explains the kinetics in both glycerol/water and trehalose solutions and therefore allows us to compare x_0 and D for the two solvents. Interesting conclusions concerning the possible underlying microscopic mechanism can then be made.

3. QUANTITATIVE MODEL

The basic assumption of the model (Agmon & Hopfield, 1983) is that ligand binding is determined by two coordinates: the ligand−iron separation, r, and an effective protein coordinate, x. It is believed that the protein influences ligand binding reactivity by modulating the out-of-plane iron

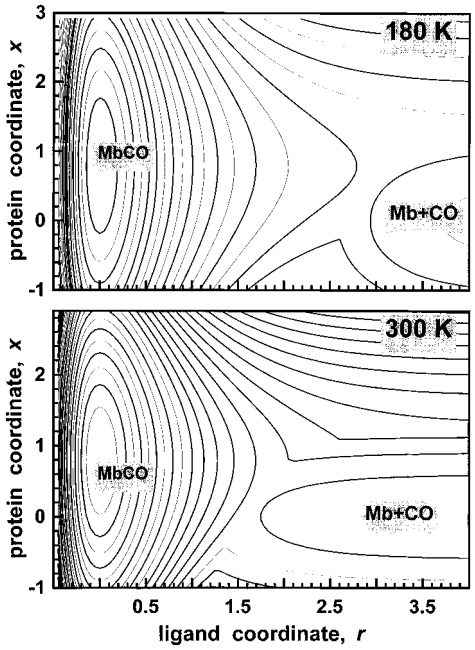

FIGURE 2: Potential surface for MbCO in trehalose at two different temperatures. $\beta = 1.5$ au^{-1}, and other parameters are in Table 1. Equipotential contours are drawn every 2 kcal/mol (=8.36 kJ/mol).

distance through its proximal-histidine linkage to the F-helix. This "proximal control" hypothesis is supported by correlations between spectroscopy and kinetics (Sage & Champion, 1996). The present study, which characterizes the protein relaxation in x, might help in testing this hypothesis.

The two-dimensional potential is constructed of intersecting Morse−exponential curves along r (for the bound−unbound states), on which a harmonic conformational potential in x is superimposed.

$$V(r,x) = \min\begin{cases} D'_e\,(e^{-2\beta r} - 2e^{-\beta r}) + {}^1/_2\, f'(x - x_0)^2, \\ \qquad\qquad\qquad\qquad \text{bound state} \\ D_e\, e^{-\beta r} - \Delta + {}^1/_2\, f x^2, \text{ pocket state} \end{cases} \quad (2)$$

The general shape of the potential is that of two wells, displaced along the protein coordinate (Figure 2). Within the proximal-control hypothesis, x_0 depicts differences in the iron equilibrium position between the bound and the deoxy states. In the first case the iron is in the porphyrin plane, while in the deoxy case it is displaced by 0.2−0.5 Å in the distal direction (Perutz *et al*., 1987; Schlichting *et al*., 1994).

The potential function, exemplified in Figure 2, generalizes the Agmon−Hopfield potential (Agmon & Hopfield, 1983) in two respects. First, the well depth (D_e) and force constant (f) may assume different values in the bound (primed) and unbound (unprimed) states. Second, several of the parameters are made temperature-dependent.

$$f = Tf_0 / \bar{T}, \qquad f' = af$$

$$\Delta = T\Delta_0 / \bar{T}$$

$$D_e = 2D'_e/(3T/\bar{T} - 1) \quad (3)$$

Here T is the actual absolute temperature of the sample whereas $\bar{T}$ is a scaling temperature. While we allow temperature-dependence of $x_0(T)$, the parameters f_0, a, Δ_0, and D'_e are assumed temperature-independent. This is essentially the same as Model B of our previous work (Agmon & Sastry, 1996). The linear temperature-dependence of the force constant, f, resembles the situation for rubber elasticity (Hill, 1960). A microscopic derivation of such a temperature-dependence is lacking.

From the potential in eq 2, it is possible to calculate a conformation-dependent barrier height, $V^{\ddagger}(x)$, as the vertical climb from $r = \infty$ to the ridgeline at $r^{\ddagger}(x)$.

$$V^{\ddagger}(x) = V(r^{\ddagger},x) - V(\infty,x) = D_e \exp(-\beta r^{\ddagger}(x)) \quad (4)$$

The second equality is obtained by equating the two forms of eq 2, which upon resubstitution yields

$$V^{\ddagger}(x)\,[2D'_e/D_e + 1 - D'_e V^{\ddagger}(x)/D_e^{\,2}] = f'(x - x_0)^2/2 - fx^2/2 + \Delta \quad (5)$$

Note that whenever $V^{\ddagger}/D_e \ll 1$ over the whole conformational range, the last term on the left-hand side (1hs) may be neglected. Then, using eq 3, the temperature-dependence of f, Δ, and D_e exactly cancels, giving

$$3V^{\ddagger}(x) \approx (a - 1)f_0\, x^2/2 - af_0\, x_0\, x + af_0\, x_0^{\,2}/2 + \Delta_0 \quad (6)$$

When $a = 1$, it reduces to a corresponding approximation in Agmon and Hopfield (1983) [eq 6]. The specific temperature-dependence assumed in eq 3 ensures that the barrier height is temperature-dependent *only* if x_0 is so.

Consider next the initial conformational distribution, $p(x,0)$. Since the sample is prepared by equilibrating bound MbCO, we assume a Boltzmann distribution for the bound state

$$p(x,0) = (f'/2\pi k_B T)^{1/2} e^{-f'(x-x_0)^2/2k_B T} = (af_0/2\pi k_B \bar{T})^{1/2} e^{-af_0(x-x_0)^2/2k_B T} \quad (7)$$

where k_B is Boltzmann's constant. This differs from Agmon and Hopfield (1983), where for $T < T_g$ equilibration was assumed to occur at T_g, the glass transition temperature. Since we find that relaxation occurs also below T_g, there should be sufficient time for the sample to equilibrate at the actual temperature of the surroundings. Taken together with the linear temperature-dependence of the force constants, one obtains an initial distribution which may depend on temperature only through x_0.

By the Franck−Condon principle, photodissociation is faster than nuclear motion. Therefore we assume that $p(x,0)$ is also the initial distribution of the photoproduct. Whenever $x_0 \neq 0$ (and/or $f' \neq f$), this distribution is out of equilibrium for the deoxy state. From eq 7, the initial distribution of barrier heights can be calculated by

$$p(V^{\ddagger}) \equiv p(x(V^{\ddagger}),0)\,|dx/dV^{\ddagger}| \quad (8)$$

Using eqs 5 and 6, one finds that

$$\frac{dV^{\ddagger}}{dx} = \frac{f'(x - x_0) - fx}{1 + (2D'_e/D_e)(1 - V^{\ddagger}/D_e)} \approx -{}^1/_3 f_0[(1 - a)x + ax_0] \quad (9)$$

Provided that the latter function varies only mildly with x, the peak location and height are approximately

$$V^{\ddagger}_{max} \approx V^{\ddagger}(x_0) \approx (2\Delta_0 - f_0 x_0^2)/6$$

$$p(V^{\ddagger}_{max}) \approx (9af_0/2\pi k_B \bar{T})^{1/2}/(f_0 x_0) \quad (10)$$

This result again coincides with the simpler model of Agmon and Hopfield (1983), and again depends on T only through x_0. Protein "collapse" in glycerol/water is manifested (Agmon & Sastry, 1996) by a decrease in $x_0(T)$. This should lead to a shift of the distribution to higher energies, an increase in its peak height, and a concominant decrease in its width.

After an initial inhomogeneous phase characterized by a static distribution of barrier heights, eq 8, the protein starts to relax. As the distribution moves downhill along the conformational coordinate x, the barrier for recombination along r increases. Nevertheless, ligand motion remains faster than that of the protein, so that one may average over the fast ligand coordinate (Rabinovich & Agmon, 1991; Agmon & Rabinovich, 1992). This "adiabatic elimination" procedure yields a one-dimensional "diffusion" (Smoluchowski) equation in the slower protein coordinate

$$\frac{\partial p(x,t)}{\partial t} = D\frac{\partial^2 p(x,t)}{\partial x^2} + \frac{D}{k_B T}\frac{\partial[(dV_{eff}/dx)p(x,t)]}{\partial x} - k(x)p(x,t) \quad (11)$$

The slow protein motion occurs on the effective one-dimensional potential

$$V_{eff}(x) = fx^2/2 \quad (12)$$

of the unbound heme while the dynamics in the fast-coordinate r are replaced by the coordinate-dependent sink term, $k(x)$, with the Arrhenius form

$$k(x) = k_0 e^{-V^{\ddagger}(x)/k_B T} \quad (13)$$

Here k_0 is a (temperature-independent) frequency factor. In a Kramers model, k_0 could depend on T through the ligand-coordinate viscosity, but here the ligand motion is assumed "ballistic" so that k_0 is a constant. $D(T)$ in eq 11 is a "diffusion coefficient" which determines the rate of protein relaxation. The protein motion depends strongly on T through this parameter.

Propagation of eq 11 generates $p(x,t)$, the distribution of deoxy protein conformations at time t, starting from $p(x,0)$ of eq 7. This introduces an x_0 dependence into the unbound heme "survival probability", $S(t)$. The latter is obtained by integrating $p(x,t)$ over the range of x's corresponding to the deoxy state

$$S(t) = \int p(x,t)\, dx \quad (14)$$

It represents the overall probability that the photodissociated heme has not recombined by time t, to be compared with the experimental transient absorption changes of the porphyrin moiety.

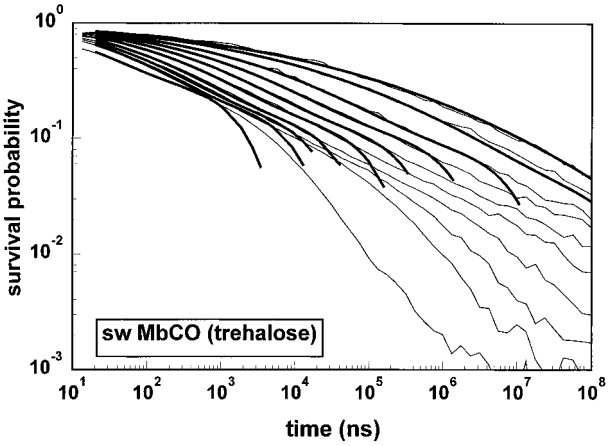

FIGURE 3: CO binding to sperm whale myoglobin in trehalose. Experimental data: thin curves (Hagen *et al*., 1995, 1996). Temperatures (top to bottom) are 105, 116, 135, 152, 170, 187, 208, 224, 241, and 297 K. Model: bold curves, with parameters collected in Table 1 and Figures 5 and 6.

Table 1: Temperature-Independent Parameters for sw MbCO Kinetics in the Two Solvents (See Eqs 2, 3, and 13)[a]

solvent	f_0	a	Δ_0 (kcal/mol)	D'_e (kcal/mol)	$\bar{T}$ (K)	k_0 (1/ns)	x_0
75% glycerol	14.65	1.2	14.5	33	505	1.5	varies
trehalose	14.65	0.8	11.0	33	505	1.0	0.79[b]

[a] The units of x_0 and f_0 depend on unspecified distance units. [b] For $T > 150$ K.

4. RESULTS

Figure 3 shows MbCO-rebinding kinetics in trehalose glass (Hagen *et al*., 1995, 1996). In comparison with the data in glycerol/water (Post *et al*., 1993), Figure 1, there is no apparent "inverse temperature effect": the reaction becomes faster with increasing temperature throughout the whole range. As we will show, this is due mostly to the absence of protein "collapse" rather than the absence of protein relaxation.

The bold curves in Figure 3 represent our fits to eqs 11 and 14 using the model of the previous section. Adjusting the solution of the partial differential equation to fit the data is facilitated by the graphical interface of a user-friendly MS Windows application for solving the spherically symmetric diffusion problem, SSDP version 1.4 (Krissinel' & Agmon, 1996). Six temperature-independent parameters were adjusted manually and collected in Table 1. In addition, x_0 and D were allowed to vary with T. The ensuing potential energy surfaces, eq 2, are shown for two temperatures in Figure 2.

Figure 4 compares the coordinate-dependent sink function, eq 13, with that of MbCO in glycerol/water. Since k_0 is very similar in the two solvents (Table 1), this is also a comparison of the coordinate-dependent barrier, $V^{\ddagger}(x)$. It is clear from the figure that even in the low-temperature regime, $T \leq 180$ K, the barrier is considerably lower for trehalose. All of the potential parameters at these temperatures are nearly the same for the two solvents, except Δ_0. Its lower value in trehalose is thus responsible for the higher reactivity there.

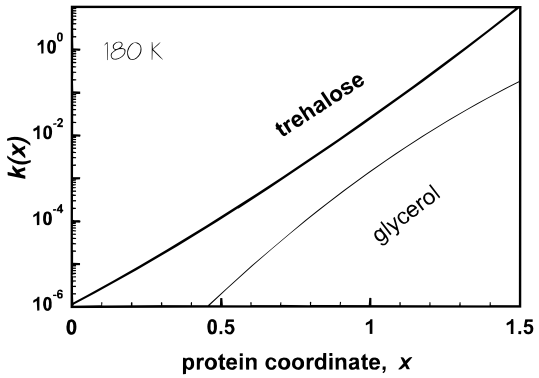

FIGURE 4: Comparison of the sink function, $k(x)$, in the two solvents.

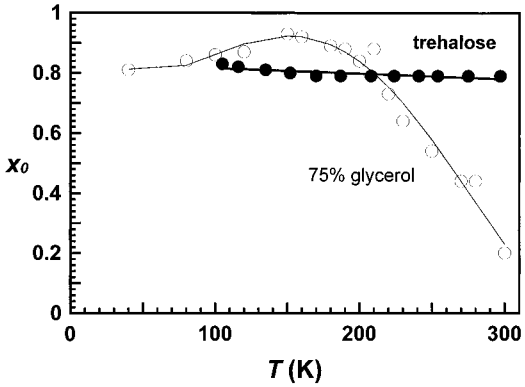

FIGURE 5: Temperature-dependence of the conformational shift, x_0, obtained from the fits shown in Figures 1 and 3. Lines are polynomial fits to guide the eye.

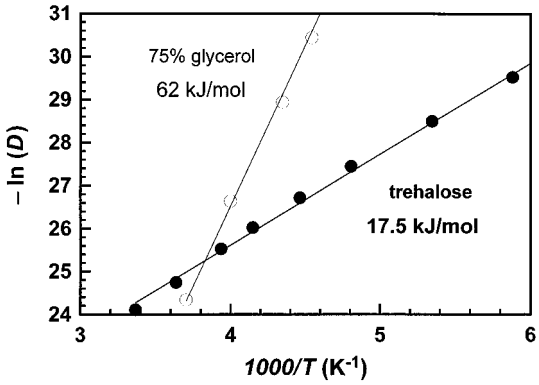

FIGURE 6: Temperature-dependence of the protein mode "diffusion coefficient", as determined from the fits in Figures 1 and 3. Note the Arrhenius behavior with the indicated activation energies.

The comparison of the conformational shifts, x_0, and conformational diffusion coefficients, D, between the two models is revealing. The temperature-dependence of the first parameter is shown in Figure 5. In 75% glycerol, x_0 decreases sharply above the solvent glass transition (ca. 190 K). This "collapse" of the conformational potential contributes a static factor to the inverse temperature effect. It is manifested in slowing down of geminate recombination during its initial inhomogeneous phase, see Figure 1. In contrast, the "collapse" phenomenon is completely prevented by trehalose, where x_0 assumes a constant value, very close to its value in 75% glycerol below 100 K.

The comparison between the diffusion coefficients is shown in Figure 6. In both solvents, $D(T)$ obeys an Arrhenius expression,

$$D(T) = D_0 \exp(-E_D/k_B T) \tag{15}$$

The pre-exponent, $\ln D_0$, is 3.35 for glycerol/water and −17.1 for trehalose. The units of D depend on the distance units, which are unspecified for the present potential. If they were in Å, D would be given in cm^2/s. In any event it is tiny compared to translational diffusion coefficients in solution. This reflects the fact that the mean square displacement for conformational change is small compared to the translational motion of small molecules. Our experience shows that variations in D_0 may be compensated, to an extent, by changes in the other parameters of Table 1. In contrast, E_D appears to be relatively robust to parameter variations. We find $E_D \approx 62$ and 17.5 kJ/mol for 75% glycerol and trehalose, respectively.

(a) The fact that D assumes a non-zero value in trehalose indicates that protein relaxation does take place in this glass.

(b) Perhaps counter-intuitively, E_D is markedly smaller in trehalose, indicating *lower* internal protein viscosity (at temperatures below the curve-crossing seen in Figure 6).

The model fits up to the time when protein relaxation terminates and the calculated $S(t)$ becomes exponential, whereas the experimental population continues to decay non-exponentially. We attribute the latter to the onset of ligand escape from the heme pocket. Our geminate model does not allow for escape, hence in the third recombination phase (after the termination of relaxation) it predicts faster rebinding rates than actually observed. The times when the theoretical and experimental curves diverge in Figures 1 and 3 are collected in Figure 7. These escape times show an Arrhenius behavior quite similar to that of $D(T)$ in Figure 6. The activation energies for escape are smaller by less than 10% as compared with E_D. Even the temperature at which the two lines cross is similar in the two figures. This similarity could indicate that ligand escape is controlled by protein relaxation, in agreement with molecular dynamics simulations (Carlson *et al*., 1996).

Finally, Hagen *et al*. (1996) have determined also the transient spectral shift for the photolyzed Mb Soret band in terms of the ratio of the first two SVD components, V_2/V_1. Assuming that a monotonic relation exists between absorption wavelength and protein conformation (Agmon & Hopfield, 1983; Agmon, 1988), one could relate the average conformation

$$\langle x \rangle \equiv \int x\, p(x,t)\, \mathrm{d}x/S(t) \tag{16}$$

obtained from propagating eq 11, to the measured V_2/V_1. We assume that

$$\langle x \rangle = a + b(V_2/V_1) + c(V_2/V_1)^2 \tag{17}$$

so that a comparison with spectral shifts depends on the parameters a, b, and c. These parameters were adjusted manually until the semiquantitative agreement of Figure 8 was obtained. Given the difficulty in an accurate determination of spectral shifts within the wide Soret band and the various corrections employed (Hagen *et al*., 1996), we believe there is no point in pursuing a fully quantitative agreement. We conclude that our model explains simultaneously both rebinding kinetics and spectral shifts as a combination of KHB and relaxation.

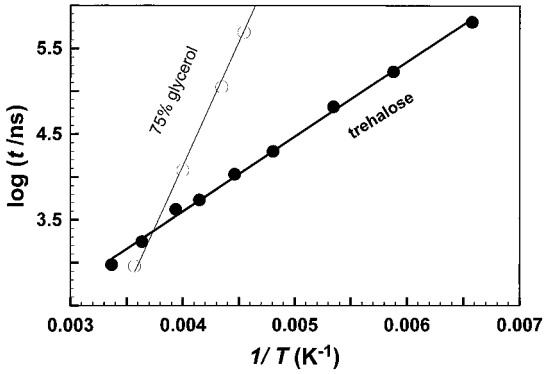

FIGURE 7: Comparison of the ligand escape times in the two solvents. Activation energies are 55 and 16.6 kJ/mol in 75% glycerol and trehalose, respectively.

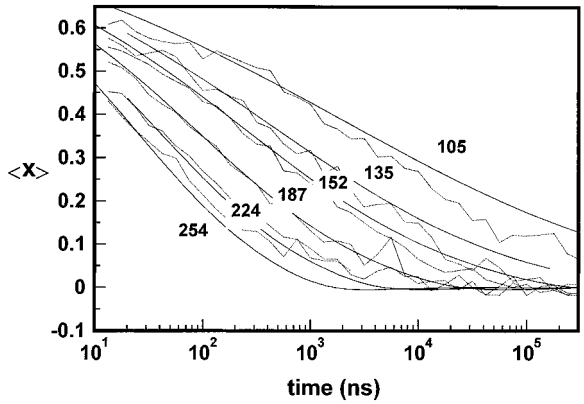

FIGURE 8: Average protein conformation obtained from the same $p(x,t)$ used to fit the kinetic data in Figure 3, full lines, is compared with the measured ratio of SVD components (Hagen *et al*., 1996), dotted lines, using eq 17 with $a = 0.48$, $b = -4$, and $c = 8$. The six indicated temperatures are in degrees kelvin.

5. DISCUSSION

5.1. Inhomogeneous Rebinding and Protein Collapse

Let us first characterize more precisely the inhomogeneous and relaxation phases in trehalose. The initial phase of geminate recombination (which might cover the whole time regime at low temperatures) is that of inhomogeneous rebinding. In agreement with Hagen *et al*. (1995, 1996), we show below that in trehalose most (but not all) of the population decays inhomogeneously even at room temperature.

The inhomogeneous phase is characterized (Austin *et al*., 1975) by a distribution of barrier heights, $p(V^{\ddagger})$. In the present model $p(V^{\ddagger})$ may be calculated from the initial distribution, eq 7, using eq 8. Figure 9 shows this static distribution as obtained from the best-fit parameters of Table 1. The peak's energy, $V^{\ddagger}_{max}$, can be estimated from eq 10. Exact and approximate values for $V^{\ddagger}_{max}$ are collected in Table 2.

Equation 10 helps rationalize the differences between the distribution in glycerol and trehalose seen in Figure 9:

(a) In 75% glycerol, $p(V^{\ddagger})$ is temperature dependent due to the decrease in x_0 with T which characterizes protein "collapse". As seen from eq 10, $V^{\ddagger}_{max}$ and $p(V^{\ddagger}_{max})$ increase with increasing T while the width of $p(V^{\ddagger})$ decreases. Thus a sizeable fraction of the slowing down in this solvent is static, and only part of the "inverse temperature effect" is dynamic. In contrast, $p(V^{\ddagger})$ is temperature independent in trehalose, which is capable of totally preventing protein collapse.

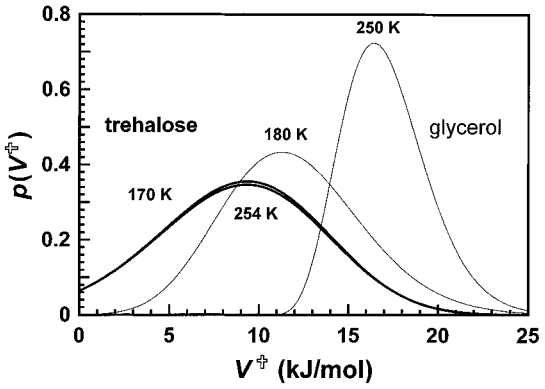

FIGURE 9: Comparison of the distribution of barrier heights, calculated from eq 8 at two temperatures for each solvent.

Table 2: Peak in the Distribution of Barrier Heights (in kJ/mol) at Two Different Temperatures (See Figure 9)

	solvent			
	75% glycerol		trehalose	
	180 K	250 K	170 K	254 K
exact	11.3	16.4	9.3	9.3
eq 10	11.7	16.8	9.0	9.0

(b) Rebinding in trehalose is faster, as evident from Figure 4. Even at low temperatures $V^{\ddagger}_{max} \approx 9$ kJ/mol, lower by 2 kJ/mol in comparison to 75% glycerol (see Table 2). Hagen *et al*. (1996) have observed a similar trend, though their $V^{\ddagger}_{max}$ in trehalose is even lower, 6.5 kJ/mol. In our model, the different low-temperature peak energies arise primarily from variations in Δ_0, which is lower in trehalose by 13.4 kJ/mol (3.5 kcal/mol, Table 1). Since Δ measures stabilization of the CO in the heme pocket [see Figure 1 of Agmon and Hopfield (1983)], we conclude that the unbound CO is stabilized in the heme pocket for glycerol/water as compared with trehalose, making its rebinding rate slower.

(c) The distribution in trehalose is wider, indicating larger protein inhomogeneity as compared with glycerol/water.

5.2. Protein Relaxation in Trehalose

The second phase of CO binding to Mb in glycerol/water involves protein relaxation (Agmon *et al*., 1994). We now demonstrate in several ways that (in contrast to eq 1) this phase is observed also in trehalose glass (a) by comparing the kinetics predicted from our model with and without relaxation; (b) by considering the density profiles, $p(x,t)$, and (c) by applying the model-independent B-function analysis (Agmon & Rabinovich, 1992; Agmon *et al*., 1994; Berlin *et al*., 1995).

Consider first the highest temperature where relaxation, if occurs, should be most prominent. Figure 10a shows the comparison between experiment and theory at room temperature. The bold and dashed curves are solutions of eq 11 with and without relaxation, respectively. In other words, we have first fitted the data using a finite value for D (Figure 6) and then repeated the calculation after resetting $D = 0$ (dashed line). From a comparison of the two curves it is clear that considerably faster rebinding would be predicted in the absence of protein relaxation.

We now demonstrate that this conclusion is independent of the model applied to fit the data. This is achieved by

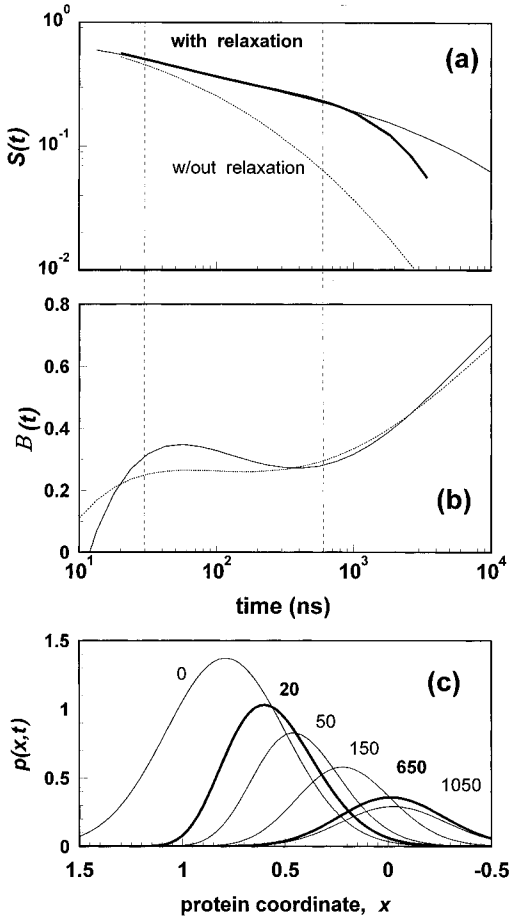

FIGURE 10: Evidence for relaxation in room temperature CO binding to sw Mb embedded in a trehalose glass. (a) Thin curve: experimental data (Hagen *et al*., 1995, 1996). Thick curve: solution to eq 11 with parameters from Table 1, see Figure 3. Dashed curve: same solution only with $D = 0$. (b) The B-function, eq 18, calculated from the experimental data in panel a by fitting it to a sixth order polynomial over the whole time regime (full curve) or up to 100 μs (dashed curve). Dotted vertical lines mark the onset (left) and termination (right) of protein relaxation. (c) The profiles, $p(x,t)$, obtained while solving for $S(t)$ of panel a. The two bold profiles correspond to the onset and termination of relaxation.

extracting the times for "onset" and "termination" of relaxation from our calculations and comparing them with a model-independent analysis. First, note how the dashed curve diverges from the experimental one at 20−30 ns. Since it was calculated under the assumption of no relaxation, it follows that this time corresponds to the "onset of protein relaxation". Second, the bold curve deviates from the experimental data around 800 ns. It was calculated from our model which includes relaxation but not ligand migration. Consequently it is reasonable to attribute the slower rebinding at $t > 800$ ns to ligand escape from the heme pocket. If, as the molecular dynamics calculations show, ligand escape is enabled by protein fluctuations the onset of ligand escape must occur somewhat after the "termination of protein relaxation". Consequently, the divergence times for the two calculations (two vertical dashed lines) mark the "onset" and "termination" of relaxation.

A model-independent determination of these times can be achieved from the B-function analysis (Agmon & Rabinovich, 1992; Agmon *et al*., 1994). The B-function is defined by

$$\mathrm{B}(t) \equiv -\mathrm{d}\ln S(t)/\mathrm{d}\ln t \qquad (18)$$

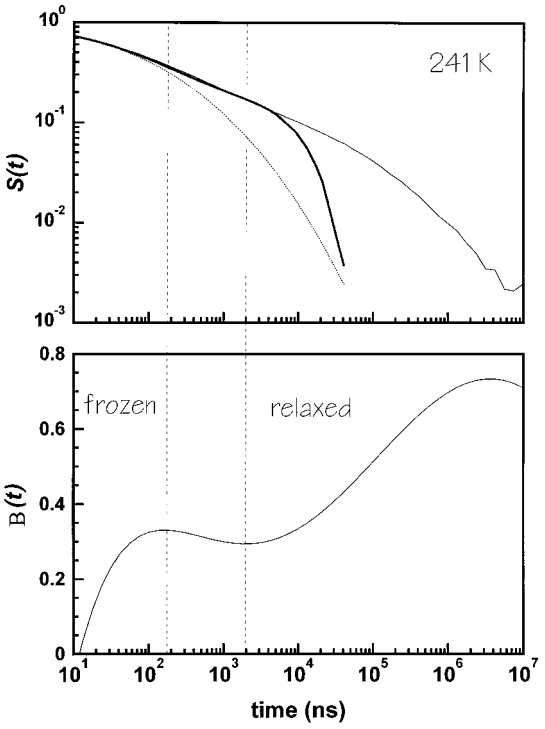

FIGURE 11: Same as Figure 10(a,b) but at a lower temperature.

As corroborated by multipulse data (Agmon *et al*., 1994), its first maximum (at t_{max}) marks the "onset" of relaxation whereas its minimum (at t_{min}) signals the "termination" of the relaxation process. The S-shaped B(t) was termed the "relaxation footprint" (Agmon *et al*., 1994).

We have calculated B(t) by fitting a sixth order polynomial to the experimental data and differentiating the polynomial analytically. This procedure is less noisy than direct numerical differentiation of the data. At room temperature, even this technique does not allow an accurate determination of B(t): by choosing different time ranges for the polynomial fits, the two B-functions of Figure 10b are generated. One can nevertheless estimate that $t_{max} \approx 20-50$ ns while $t_{min} \approx 600$ ns, both in reasonable agreement with the prediction from our model with and without relaxation, Figure 10a.

The third panel in Figure 10 shows the temporal evolution of the density profile, the solution of eq 11, whose zeroth and first moments, $S(t)$ and $\langle x \rangle$, were used to fit the population decay and spectral shift. The profiles at 20 and 650 ns indeed correspond to what one understands by "onset" and "termination" of relaxation: at 20 ns $p(x,t)$ first moves out of the "envelope" of the initial distribution, $p(x,0)$. After 650 ns, it no longer shifts but only diminishes in amplitude. By the time $\langle x \rangle$ reaches the bottom of the potential, the observation time window becomes large as compared with protein fluctuation times so that the distribution is both relaxed and homogenized.

To verify that the agreement shown is not due to inaccuracies in B(t), we performed the analysis at a lower temperature (241 K), where B(t) can be determined more accurately. Figure 11 shows a nice agreement between the times at which the calculated $S(t)$ with and without relaxation diverges from the experimental data (upper panel) and the extrema t_{max} and t_{min} of B(t) in the lower panel (vertical dotted lines). Thus at 241 K relaxation begins already at ≈150 ns and ends by a few μs.

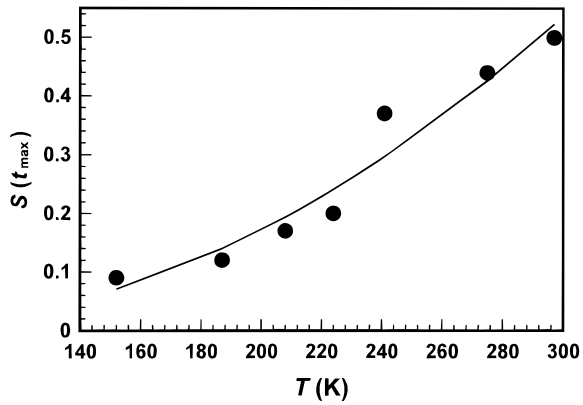

FIGURE 12: Unbound fraction of sw MbCO(trehalose) at the onset of protein relaxation, t_{max}. $1 - S(t_{max})$ is the fraction that rebinds inhomogeneously.

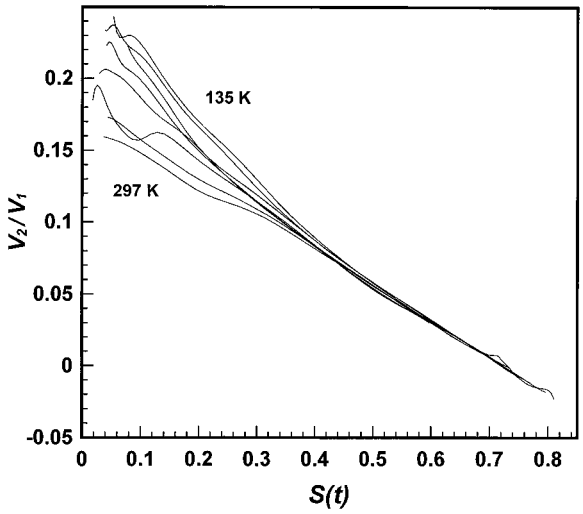

FIGURE 13: Universal plot of shifts vs rebinding for MbCO in trehalose glass (Hagen *et al*., 1996). Temperatures (top to bottom) are 135, 152, 187, 208, 224, 254, 275, and 297 K.

To determine the percentage of the population that recombines inhomogeneously, prior to the onset of relaxation, we first performed the B-function analysis on the experimental population decay data at several temperatures to obtain t_{max}. From it, $S(t_{max})$ was estimated as seen in Figure 12. $1 - S(t_{max})$ represents the fraction of the initial population which recombines inhomogeneously. This fraction is around 50% at room temperature and increases with decreasing T. As stated at the outset of this section, most of the population does indeed react inhomogeneously. Nevertheless, relaxation of the minority is clearly detected.

5.3. Universal KHB Correlation

An established procedure for assessing the extent of inhomogeneity is to plot the spectral shift, V_2/V_1, versus the unbound fraction, $S(t)$. A "universal curve" (independent of T) is taken as evidence for KHB (Agmon, 1988; Šrajer *et al*., 1991). Figure 3 of Hagen *et al*. (1996) shows this correlation for the original data. At large $S(t)$ values (small t) the universal correlation is apparent, but at smaller $S(t)$ (longer times) the increasing noise obscures any systematic trends in the data. Smoothing the data by a simple iterative two-point averaging subroutine produced Figure 13. In now becomes apparent that at small $S(t)$ the curves fan out systematically, lower curves corresponding to higher T. If divergence from the universal curve is taken as evidence for relaxation, one concludes that relaxation begins at larger S for higher T. For example, the curves for $T = 187$ and 208 K diverge around $S = 0.2$ whereas those for $T = 275$ and 295 K diverge around $S = 0.4$. These values are in qualitative agreement with the temperature dependence of $S(t_{max})$ in Figure 12.

It is difficult to perform the same analysis on the glycerol/water data (Figure 1) which appears too noisy. However, it is clear by inspection of Figure 1b that at room temperature, for example, most of the population reacts from a relaxed state. This is not due to faster relaxation in glycerol/water. To the contrary, the onset of relaxation was estimated (Agmon *et al*., 1994) to occur around 50−150 ns in this solvent as opposed to 20−30 ns in trehalose. The *faster* relaxation times in trehalose are in accord with the lower value of E_D, Figure 6. The large fraction of inhomogeneous rebinding in the trehalose glass as compared with 75% glycerol is rather due to the higher Mb reactivity in trehalose as evidenced, for example, by the lower peak energy, $V^{\ddagger}_{max}$, in the distribution of barrier heights (Figure 9 and Table 2). Thus in trehalose a larger fraction of the population recombines during a shorter inhomogeneous phase.

5.4. Protein Relaxation Is an Internal Process

Figure 6 indicates that the intrinsic viscosity in trehalose is considerably *lower* than in glycerol/water, in spite of the tremendous increase in external viscosity. This agrees with our earlier study of this reaction in 75% glycerol/water solutions (Agmon & Sastry, 1996), where $D(T)$ was found to obey an Arrhenius relation with the *same* activation energy both below and above the solvent T_g (see Figure 6). The fact that the relaxational rate is insensitive to the glass transition indicates that the relaxation process is intrinsic, and decoupled from the protein surface.

A similar conclusion was made by Doster and co-workers, who found that the innermost barrier in glycerol/water solutions is considerably lower than the activation energies for solvent relaxation processes, such as deduced from solvent viscosity (Doster *et al*., 1993). This also agrees with recent spectral diffusion hole-burning studies in the millikelvin range (Gafert *et al*., 1995) which indicate that the porphyrin is quite effectively shielded by the protein from the surrounding host matrix. In HbCO(trehalose) one still observes an inverse temperature effect, though it is much reduced compared to HbCO(glycerol/water) (Gottfried *et al*., 1996). The reduced effect must be due to the absence of protein collapse in trehalose, with the remainder due to protein relaxation. The inversion temperature is 140 K in trehalose, compared with 180 K in glycerol/water, suggesting a smaller activation energy for protein relaxation in the trehalose glass. All of these observations support the hypothesis that the protein relaxation which slows CO rebinding is an intrinsic process.

5.5. Are Proteins Like Glasses?

As already mentioned in the Introduction, several dynamic studies of heme proteins suggest that protein relaxations are similar to the primary, α-relaxation of glasses (Iben *et al*., 1989; Frauenfelder *et al*., 1991; Parak & Frauenfelder, 1993). In analogy to some of the glass-forming systems (Green *et al*., 1994), it was suggested that protein relaxation in MbCO

should have the following characteristics: (a) No relaxation below the solvent glass transition, T_g, due to a big jump in the internal viscosity (Austin *et al*., 1975; Hagen *et al*., 1995); (b) Stretched-exponential relaxation near T_g; and (c) Non-Arrhenius relaxation rate constants (Steinbach *et al*., 1991).

In our model no assumptions concerning the time-dependence of the relaxation process are made only on the form of the underlying effective potential. The fundamental protein relaxation process that emerges from the model shows none of the characteristics ascribed (incorrectly, perhaps) to glassy behavior:

(a) The diffusional relaxation rate, $D(T)$, shows no breaks near the solvent T_g.

(b) Sub-10 s relaxation is observed for $T > 150$ K in both glycerol/water ($T_g \approx 190$ K) and trehalose [T_g is 387 K for anhydrous trehalose (Crowe *et al*., 1996)].

(c) Diffusional relaxation on a harmonic potential, eq 12, is purely exponential. Its non-exponentiality comes only from coupling to the binding reaction (Agmon & Sastry, 1996).

(d) The temperature-dependence of $D(T)$ is closely Arrhenius, both in glycerol/water and trehalose, over the whole accessible temperature range.

Does our model contradict the expected glassy behavior of a protein? To answer this question, let us relate some of the more recent work on the thermodynamics of proteins and glasses. (a) Recently, DSC measurements have been performed on hydrated Mb (Green *et al*., 1994; Sartor *et al*., 1994, 1995). In contrast to simple glasses, these samples show no sign for a characteristic protein T_g but rather a broad range of protein relaxation processes, commencing around 150 K. It seems that all relaxation processes faster than 10 s contribute to the configurational free energy, without showing an abrupt increase characteristic of the glass→liquid transition (Sartor *et al*., 1994). (b) Glass relaxation is not necessarily non-Arrhenius in T and non-exponential in t. It is nowadays realized that an inhomogeneous distribution of environments, each characterized by different exponential relaxation rates, can lead to an averaged non-exponential relaxation function (Richert, 1994; Ediger *et al*., 1996).

Therefore, irrespective of whether proteins behave like glasses or not, it appears that the *ad-hoc* assumption that they relax in a non-exponential and non-Arrhenius fashion (Steinbach *et al*., 1991) is not necessarily found on a microscopic scale.

5.6. Raman Evidence for Relaxation, Dehydration, and Collapse

Interesting conclusions concerning the structure and reactivity of heme proteins may be drawn from Raman studies of the iron−histidine (Fe−His) stretch, in the region of 220−230 cm^{-1} (Friedman *et al*., 1982). The following sequence of observations show that, in contrast to glycerol/water solutions, trehalose preserves the structure and reactivity of Mb and prevents dehydration of the heme pocket:

(1) Higher Fe−His frequencies correlate with higher heme affinity and reactivity. Friedman and co-workers have established that species with high affinity hemoglobin, the more reactive quaternary R-state and generally conditions that favor the R-state (e.g., high pH) all correlate with *higher* Fe−His frequencies (Friedman *et al*., 1983).

(2) The photoproducts of both HbCO (Scott *et al*., 1983) and MbCO (Sassaroli *et al*., 1986) are blue-shifted with respect to the corresponding deoxy state by a few wavenumbers. Subsequent to HbCO photolysis, the Fe−His frequency red-shifts (Scott *et al*., 1983). This can be interpreted as evidence for a reactive photoproduct conformation relaxing toward the less reactive equilibrium deoxy conformation, spectroscopically observable due to correlation between spectral shifts and protein conformations.

(3) The shift between the characteristic Fe−His frequencies of deoxy-Mb and photoproduct MbCO in 75% glycerol/water (Sage *et al*., 1995) [Figure 5] decreases with increasing temperature in a manner resembling the dependence of x_0 on T depicted in Figure 5. This could represent "protein collapse".

(4) In room temperature trehalose, band III of photodissociated MbCO is around 765 nm (the same as at 10 K) and the Fe−His frequency around 224 cm^{-1} (even higher than in 90% glycerol) (Peterson *et al*., 1997). This Fe−His frequency is among the highest values observed for Mb. This indicates (a) absence of protein collapse in trehalose and (b) enhanced reactivity as compared even with low-temperature glycerol glasses, in agreement with Figure 4 above.

(5) The deoxy-Mb Fe−His frequency is red shifted by 3 cm^{-1} in 75% glycerol/water (219 cm^{-1}) as compared with aqueous buffer (222 cm^{-1}), indicating glycerol-induced protein structural change (Sage *et al*., 1995).

(6) In a His(64)Leu mutant that cannot bind water in the distal heme pocket, the Fe−His band in both water and glycerol/water occurs at the same frequency as the band of the native protein in glycerol solutions (Christian *et al*., 1996). This indicates that the structural change induced by glycerol could involve dehydration of the heme pocket.

5.7. Internal Water Hypothesis

Solvents may affect proteins through viscosity (Ansari *et al*., 1992) and osmotic pressure (Rand, 1992). The latter determines the hydration state of the protein. It appears that the surface hydration layer and the few internal water molecules are vital to normal protein function, conferring to it its internal stability and flexibility (Doster *et al*., 1986). As water molecules leave the heme pocket, the ligand entry channel, and possibly other sites, the hydrogen bonds to water are replaced by stiffer intramolecular hydrogen bonds, leading to diminished internal mobility.

Therefore the higher internal mobility in trehalose, depicted by the lower E_D value as compared to glycerol solutions (Figure 6), could be explained if trehalose protects against the loss of internal water molecules. This might arise from its higher T_g, causing it to glassify at lower concentrations that the other sugars (Green & Angell, 1989; Crowe *et al*., 1996) before its osmotic pressure rises to sufficiently high values necessary for driving out internally bound water molecules. The higher E_D in 75% glycerol could be understood if glycerol, as the Raman data indicate, dehydrates the heme pocket.

In contrast, the ability of trehalose to prevent protein collapse could be due either to retention of internal water molecules or to its increased viscosity. Likewise, enhanced collapse in glycerol/water solutions above the solvent T_g might arise from an increasing osmotic pressure or decreasing

viscosity with increasing *T*. It would be interesting to differentiate between the two effects experimentally.

6. CONCLUSION

Geminate rebinding of CO to myoglobin differs substantially between trehalose and glycerol/water solutions. In the present work, rebinding kinetics in both environments were quantitatively analyzed using a model that involves conformational diffusion on an effective, temperature-dependent potential. Presently, this constitutes the only treatment that successfully fits the complicated time course of this reaction during both inhomogeneous and relaxational phases by solving an equation of motion. The approach provides us with the temperature dependence of the effective potential and the conformational diffusion coefficient that help interpret the role of the solvent in this fundamentally important process. In particular, it sheds light on the mechanism by which trehalose preserves protein activity under dehydrated conditions.

We have previously suggested (Agmon & Sastry, 1996) that the inverse temperature effect observed in glycerol/water is due partly to dynamic relaxation, which increases the barrier height for rebinding, but partly to a static effect, "protein collapse", which leads to smaller variations between the equilibrium conformations of the bound and deoxy states at elevated temperatures. The activation energy for relaxation (conformational diffusion) is large and insensitive to the solvent glass transition, implying that it is an internal process.

In trehalose, which forms a glass well above room temperature, most of the rebinding occurs during the inhomogenous phase. This is not due to slowing down of protein relaxation but rather to the ability of trehalose to completely prevent protein collapse. As a result, rebinding becomes faster and takes place mostly before the onset of relaxation. The fraction that does relax, relaxes faster than in glyercol/water. The fact that, in spite of the tremendous increase of external viscosity in trehalose, the internal viscosity *decreases* corroborates the conclusion that this relaxation process is internal and mostly decoupled from the protein surface. Yet, assuming proximal control, the relaxation is sufficiently extensive to couple the proximal and distal sides of the heme, allowing ligand escape after its termination.

Possible molecular origin for these observations might involve viscosity and dehydration effects. It is hard to understand the enhanced internal mobility of myoglobin embedded in a trehalose glass without recourse to the internal water hypothesis. It is less clear whether the prevention of collapse is due to enhanced viscosity or reduced dehydration. It is even less obvious which of these effects should correlate with the anhydrobiotic properties of the glass. A comparative study of different glasses could be revealing.

ACKNOWLEDGMENT

We thank John F. Carpenter, William A. Eaton, Ron Elber, Joel M. Friedman, Gyan P. Johari, Stephen J. Hagen, and Erwin Mayer for discussions and comments. We are grateful to Stephen J. Hagen and Wolfgang Doster for the MbCO data in trehalose and glycerol/water solutions.

REFERENCES

Agmon, N. (1988) *Biochemistry 27*, 3507−3511.

Agmon, N., & Hopfield, J. J. (1983) *J. Chem. Phys. 79*, 2042−2053.

Agmon, N., & Rabinovich, S. (1992) *J. Chem. Phys. 97*, 7270−7286.

Agmon, N., & Sastry, G. M. (1996) *Chem. Phys. 212*, 207−219.

Agmon, N., Doster, W., & Post, F. (1994) *Biophys. J. 66*, 1612−1622.

Ansari, A., Jones, C. M., Henry, E. R., Hofrichter, J., & Eaton, W. A. (1992) *Science 256*, 1796−1798.

Ansari, A., Jones, C. M., Henry, E. R., Hofrichter, J., & Eaton, W. A. (1994) *Biochemistry 33*, 5128−5145.

Austin, R. H., Beeson, K. W., Eisenstein, L., Frauenfelder, H., & Gunsalus, I. C. (1975) *Biochemistry 14*, 5355−5373.

Berlin, Y. A., Fischer, S. F., Chekunaev, N. I., & Goldanskii, V. I. (1995) *Chem. Phys. Lett. 200*, 369−385.

Campbell, B. F., Chance, M. R., & Friedman, J. M. (1987) *Science 238*, 373−376.

Carlson, M. L., Regan, R. M., & Gibson, Q. H. (1996) *Biochemistry 35*, 1125−1136.

Carpenter, J. F., & Crowe, J. H. (1989) *Biochemistry 28*, 3916−3922.

Carpenter, J. F., Crowe, L. M., & Crowe, J. H. (1987) *Biochim. Biophys. Acta 923*, 109−115.

Cheng, X., & Schoenborn, B. P. (1990) *Acta Crystallogr. B 46*, 195−208.

Cheng, X., & Schoenborn, B. P. (1991) *J. Mol. Biol. 220*, 381−399.

Christian, J. F., Unno, M., Sage, J. T., Sligar, S. G., Chien, E., & Champion, P. M. (1996) *Biophys. J. 70*, A336.

Crowe, J. H., Hoekstra, F. A., & Crowe, L. M. (1992) *Annu. Rev. Physiol. 54*, 579−599.

Crowe, L. M., Reid, D. S., & Crowe, J. H. (1996) *Biophys. J. 71*, 2087−2093.

Doster, W., Bachleitner, A., Dunau, R., Hiebl, M., & Lüscher, E. (1986) *Biophys. J. 50*, 213−219.

Doster, W., Kleinert, T., Post, F., & Settles, M. (1993) in *Protein−Solvent Interactions* (Gregory, R. B., Ed.) p 375, Marcel Dekker, New York.

Ediger, M. D., Angell, C. A., & Nagel, S. R. (1996) *J. Phys. Chem. 100*, 13200−13212.

Edsall, J. T., & McKenzie, H. A. (1983) *Adv. Biophys. 16*, 53−183.

Franzen, S., Bohn, B., Poyart, C., & Martin, J. L. (1995) *Biochemistry 34*, 1224−1237.

Frauenfelder, H., Sligar, S. G., & Wolynes, P. G. (1991) *Science 254*, 1598−1603.

Friedman, J. M. (1985) *Science 228*, 1273−1280.

Friedman, J. M., Rousseau, D. L., & Ondrias, M. R. (1982) *Annu. Rev. Phys. Chem. 33*, 471−491.

Friedman, J. M., Scott, T. W., Stepnoski, R. A., Ikeda-Saito, M., & Yonetani, T. (1983) *J. Biol. Chem. 258*, 10564−10572.

Gafert, J., Pschierer, H., & Friedrich, J. (1995) *Phys. Rev. Lett. 74*, 3704−3707.

Gottfried, D. S., Peterson, E. S., Sheikh, A. G., Wang, J., Yang, M., & Friedman, J. M. (1996) *J. Phys. Chem. 100*, 12034−12042.

Green, J. L., & Angell, C. A. (1989) *J. Phys. Chem. 93*, 2880−2882.

Green, J. L., Fan, J., & Angell, C. A. (1994) *J. Phys. Chem. 98*, 13780−13790.

Hagen, S. J., Hofrichter, J., & Eaton, W. A. (1995) *Science 269*, 959−962.

Hagen, S. J., Hofrichter, J., & Eaton, W. A. (1996) *J. Phys. Chem. 100*, 12008−12021.

Hill, T. L. (1960) *An Introduction to Statistical Mechanics*, Addison-Wesley, Reading, MA.

Iben, I. E. T., Braunstein, D., Doster, W., Frauenfelder, H., Hong, M. K., Johnson, J. B., Luck, S., Ormos, P., Schulte, A., Steinbach, P. J., Xie, A. H., & Young, R. D. (1989) *Phys. Rev. Lett. 62*, 1916−1919.

Krissinel', E. B., & Agmon, N. (1996) *J. Comput. Chem. 17*, 1085−1098.

Lambright, D. G., Balasubramanian, S., & Boxer, S. G. (1991) *Chem. Phys. 158*, 249−260.

Lounnas, V., Pettitt, B. M., Findsen, L., & Subramaniam, S. (1992) *J. Phys. Chem. 96*, 7157−7159.
Lounnas, V., Pettitt, B. M., & Phillips, G. N., Jr. (1994) *Biophys. J. 66*, 601−614.
Nienhaus, G. U., Mourant, J. R., & Frauenfelder, H. (1992) *Proc. Nat. Acad. Sci. U.S.A. 89*, 2902−2906.
Parak, F., & Frauenfelder, H. (1993) *Physica A (Amsterdam) 201*, 332−345.
Perutz, M. F., Fermi, G., Luisi, B., Shaanan, B., & Liddington, R. C. (1987) *Acc. Chem. Res. 20*, 309−321.
Peterson, E., Perez, J., Levin, L., & Friedman, J. M. (1997) (submitted for publication).
Petrich, J. W., Lambry, J.-C., Kuczera, K., Karplus, M., Poyart, C., & Martin, J.-L. (1991) *Biochemistry 30*, 3975−3987.
Post, F., Doster, W., Karvounis, G., & Settles, M. (1993) *Biophys. J. 64*, 1833−1842.
Prestrelski, S. J., Tedeschi, N., Arakawa, T., & Carpenter, J. F. (1993) *Biophys. J. 65*, 661−671.
Rabinovich, S., & Agmon, N. (1991) *Chem. Phys. Lett. 182*, 336−342.
Rand, R. P. (1992) *Science 256*, 618.
Richert, R. (1994) *J. Non-Cryst. Solids 209*, 172−174.
Rupley, J. A., & Careri, G. (1991) *Adv. Protein Chem. 41*, 37−172.
Sage, J. T., & Champion, P. M. (1996) in *Comprehensive Supramolecular Chemistry* (Suslick, K. S., Ed.) Vol. 5, Chapter 6, pp 171−218, Pergamon, New York.
Sage, J. T., Schomacker, K. T., & Champion, P. M. (1995) *J. Phys. Chem. 99*, 3394−3405.
Sartor, G., Mayer, E., & Johari, G. P. (1994) *Biophys. J. 66*, 249−258.
Sartor, G., Hallbrucker, A., & Mayer, E. (1995) *Biophys. J. 69*, 2679−2694.
Sassaroli, M., Dasgupta, S., & Rousseau, D. L. (1986) *Biophys. Chem. 261*, 13704−13713.
Schlichting, I., Berendzen, J., Phillips, J. G. N., & Sweet, R. M. (1994) *Nature 371*, 808−812.
Scott, T. W., Friedman, J. M., Ikeda-Saito, M., & Yonetani, T. (1983) *FEBS Lett. 158*, 68−72.
Šrajer, V., Reinisch, L., & Champion, P. M. (1991) *Biochemistry 30*, 4886−4895.
Steinbach, P. J., Ansari, A., Berendzen, J., Braunstein, D., Chu, K., Cowen, B. R., Ehrenstein, D., Frauenfelder, H., Johnson, J. B., Lamb, D. C., Luck, S., Mourant, J. R., Nienhaus, G. U., Ormos, P., Philipp, R., Xie, A., & Young, R. D. (1991) *Biochemistry 30*, 3988−4001.
Tian, W. D., Sage, J. T., Šrajer, V., & Champion, P. M. (1992) *Phys. Rev. Lett. 68*, 408−411.

BI9626057